Preprint: This is a non-peer-reviewed preprint submitted to EarthArXiv.

COMPUTATIONAL MODELING OF CLIMATE CHANGE IMPACTS ON FLOOD INFLOWS USING REMOTE SENSING AND SWAT: A CASE STUDY OF BAN CHAT RESERVOIR, NORTHERN VIETNAM

Vu Thi Phuong Thao
Faculty of Environment
Hanoi University of Mining and Geology
Hanoi, Vietnam
vuthiphuongthao@humg.edu.vn

Le Vu Anh
Department of Mathematics and Computer Science
Beloit College
Beloit, WI, USA
leav@beloit.edu

ABSTRACT

This study examines the changes in land cover and three water quality indicators (chlorophyll-*a*, colored dissolved organic matter, turbidity) using Sentinel-2 imagery in the Ban Chat hydropower area in Northern Vietnam during the period of 2016–2024. To assess the potential impact of flood flows into the Ban Chat reservoir, key information is extracted from remote sensing data, which is the Vietnam climate change scenarios published in 2020, and the SWAT hydrological model is also utilized. The obtained results indicate that: (1) there is a relationship among land cover, chlorophyll-*a*, colored dissolved organic matter, and turbidity in the study area; (2) the impacts of climate change on flood flow into the Ban Chat reservoir depict complex fluctuations and differed significantly depending on the simulated time and climate change scenarios. The SWAT hydrological model of the flood flow change calculation results show an increasing trend during most periods.

Keywords remote sensing · land cover · water quality indicator · climate change scenario · flood flow · reservoir

1 Introduction

Climate change has caused extreme weather events, with increased natural disasters. Globally, the trend has become more severe, prevalent, and irregular, making it increasingly difficult to ensure sustainable water resource management (Ostfeld et al. [2012]). Climate change and human interference impact the hydrology of small watersheds, as well as a substantial alteration of river flows, especially the overland flows (4/5 decrease) and the base flows (2/3 decrease), which would consequently result in important implications for terrestrial ecosystems and human well-being. Runoff in most tropical zones has increased due to extreme rainfall frequencies (Santos et al. [2014];

Yang et al. [2019]; Zhai et al. [2020]). Climate change in Vietnam is becoming more and more serious, directly affecting surface flows for 108 river basins consisting of 3,450 rivers and streams with a length of 10 km or more (Ministry of Natural Resources and Environment (MONRE) [2020]). In recent years, Vietnam's surface flows have been increasingly changing abnormally with droughts and floods occurring more and more severely (Ministry of Natural Resources and Environment (MONRE) [2020]). In this context, it is necessary to predict the extent of flow changes in the future when climate change occurs in different scenarios as well as the resilience of river basins to improve their ability to adapt to climate change and limit vulnerabilities caused by climate change. Land cover, 03 reservoir water indicators (chlorophyll content (Chl_a), colored dissolved organic matter (CDOM), and Turbidity (Turb)) are important keys in river basin research. The classification of remote sensing image types allows one to determine the land cover object changes (Franklin and Wulder [2002]; Alvarez et al. [2003]; Jensen [2005]; Hung et al. [2016]; Datta [2018]; Hung et al. [2021]; Thao et al. [2024]) proposed three main groups of remote sensing image classifications, including pixel-wise classification, subpixel-wise classification, and object-based classification. Lu and Weng (2007), Li et al. (2014), and Hung et al. (2021a) developed new methods for this purpose (Lu and Weng [2007]; Li et al. [2014]; Hung et al. [2021]).

Application of remote sensing technology in water quality assessment has been widely applied widely, based on the relationship between the optical properties of water and water quality parameters such as Chl_a, total suspended matter (TSS), Turb, Secchi depth and CDOM can be measured using remote sensing techniques (Bukata et al. [1981]; Vertucci and Likens [1989]; Gitelson [1992]; Jensen [2000]; Kallio et al. [2001]; Dekker et al. [2001]; Giardino et al. [2007]; Olmanson et al. [2008]; Hunter et al. [2010]). The Sentinel-2 remote sensing imagery is suitable for estimating Chl_a, CDOM in water bodies and tracking the spatial and temporal dynamics in the lakes (European Space Agency (ESA) [2015]; Du et al. [2016]; Kutser et al. [2016]; Ave and Alikas [2018]; Katlane et al. [2020]; Pahlevan et al. [2020]; Aranha et al. [2022]).

Recently, remote sensing data can become a solution for TSS/ Turb monitoring with large area observation and fast data accumulation. Nowadays, with the availability of Sentinel-2 with high spatial resolution (up to 10 meters) and high revisit time (up to 5 days), it will be easier to observe TSS/Turb concentration (Bioresita et al. [2018]). The concentration and distribution of TSS/Turb can be observed through Sentinel-2 satellite imagery using visible channels. The visible bands are used to determine TSS/Turb by regression analysis of band ratio. The distribution patterns of TSS/Turb detected using remote sensing employ algorithms capable of transforming pixel values into estimates of TSS/Turb concentration (Katlane et al. [2020]; Nguyen et al. [2020]; Mukhtar et al. [2021]; Riza et al. [2024]). Besides, to estimate concentrations of chlorophyll a and cyanobacteria as well as turbidity from MERIS sensor onboard ENVISAT satellite using semi-empirical bio-optical models (Potes et al. [2011]; Potes et al. [2012]), applied for Sentinel-2 imagery (Potes et al. [2018]).

The study by Västilä et al. [2010] and Van et al. [2012] studied the flows of the Mekong River basin; the other study by Ty et al. [2012] studied the flows of the Srepok River Basin while Nam et al. [2012] studied the flows of Thu Bon River Basin, etc. These studies mainly focused on analyzing flow variations among inter-year or inter-season to supply input data for hydraulic models by using numerical analyses. Other studies have focused on assessing the impact of land cover changes on the river basin flows (Nhu and Son [2009]; Trang [2009]; Hanh [2010]). At the same time, rain–runoff models have been deployed to simulate land cover changes by using precipitation scenarios of different basins (Trang [2009]). In several recent decades, remote sensing technology has proved to be a very useful tool in managing water resources, by providing essential data for

hydrological simulation models (Rango [1994] and Pietroniro and Prowse [2002]). This technology can provide multi-time and high–frequency data that is crucial in addressing the problems of data density, frequency, and quality that can limit hydrological models' accuracy (Sheffield et al. [2018]). Remote sensing data can reveal crucial information about rainfall, land cover, evapotranspiration, and topographic numerical analysis, which is an important input for hydrological flow modeling (Pietroniro and Prowse [2002]). It can also be used to accurately estimate and identify flood zones and water depths, making it an important tool for modern flood management (Smith [1997]; Wang [2015]). This direction is necessary for studying the method by combining remote sensing data and numerical models to simulate flood flows into key reservoirs (Jasrotia et al. [2002]).

2 Materials and Methods

2.1 Study Area

The study was conducted in the Ban Chat reservoir located in Lai Chau province, northern Vietnam, as shown in Figure 1. The basin spans between coordinates 15°01'36" to 15°50'30" N and 107°31'03" to 108°03'38" E, covering a surface area of 2,190 km2. The reservoir is part of the Nam Mu River basin, spanning approximately 181 km from Phong Tho district, with an elevation of 700 m in the Northwest–Southeast direction. The basin has total annual flows of 4.144 billion m3/year, with an average flow rate of 80l/s, and a flow modulus of 2% during the flood season. The flow slope is small, and the average flow rate is 50 l/s.

The topography of the basin is mountainous, characterized by mountain ranges of 1,500 m high. The soils are mainly red and yellowish. The average annual rainfall in the basin catchment is 2,105 mm/year. There are two distinct seasons, a dry season from October to March followed by a rainy season from May to September. The dry season receives approximately 20–25% of the total annual rainfall (Hung [2021]).

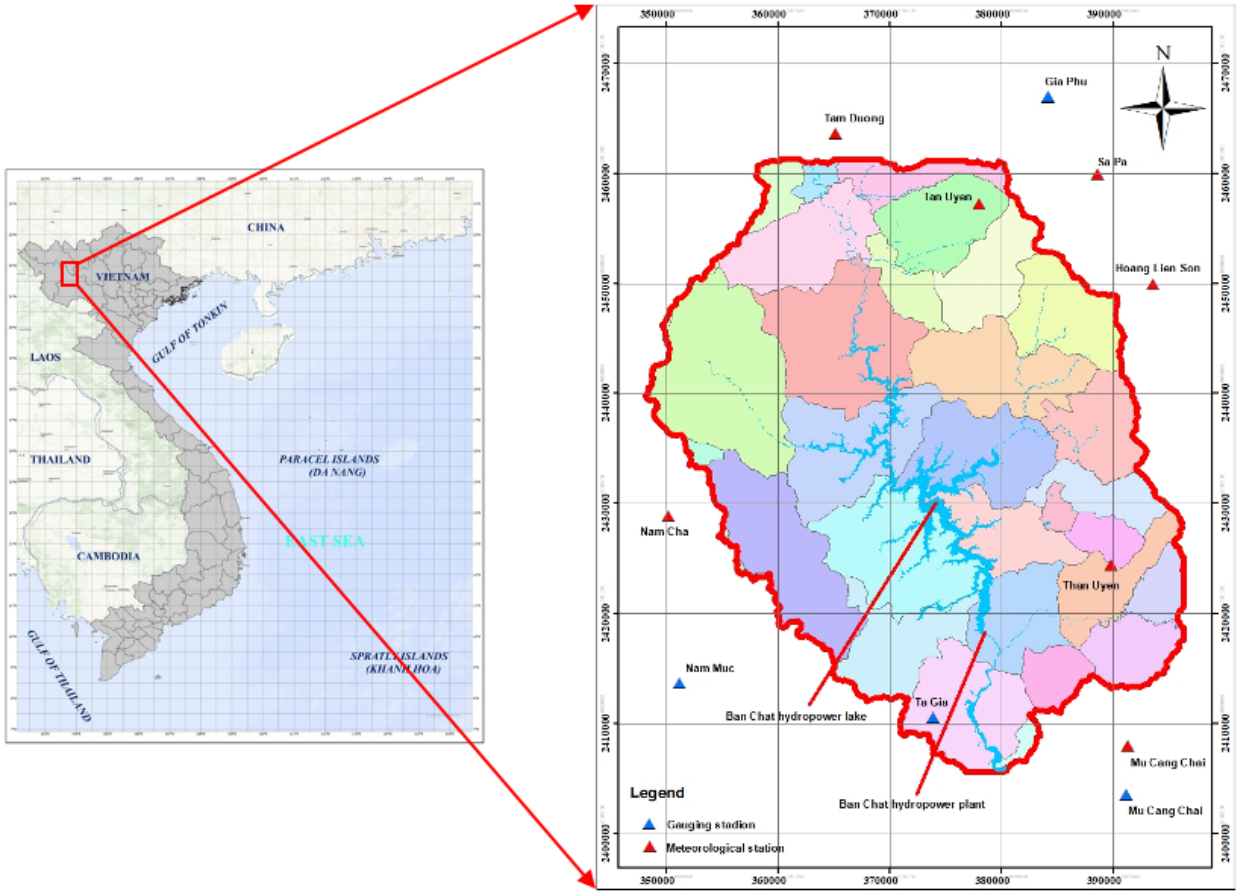

Figure 1: Map of the study area.

2.2 Input Data

Sentinel-2 Multispectral Imager's (MSI) data in Single Look Complex (SLC) format at level 1 were utilized for monitoring land cover in the years 2016, and 2024 as well as Chl_a, CDOM, and Turb during the period of 2016-2024. Sentinel-2 images used in this study were downloaded from the website of The United States Geological Survey (USGS): https://earthexplorer.usgs.gov. Of the total 13 channels of Sentinel-2 images collected, 10 image bands (band 2, 3, 4, 5, 6, 7, 8, 8A, 11, and 12) were selected for inclusion in the classification; bands 1, 9 and 10 were used for atmospheric correction (Tuan et al. [2022]). Note that the estimated Sentinel-2 remote sensing data for each year was generated by combining all Sentinel-2 images acquired for that specific year. For example, the estimated Sentinel-2 data for 2016 was generated by combining all Sentinel-2 images from 1st January 2016 to 31st December 2016. Besides, using the average value from analyzing field samples during 12 months of the year 2023 as a correlation to calculate the Chl_a, CDOM, and Turb contents in water.

Note that the estimated Sentinel-2 remote sensing data for each year was generated by combining all Sentinel-2 images acquired for that specific year. For example, the estimated Sentinel-2 data for 2016 was generated by combining all Sentinel-2 images from 1st January 2016 to 31st December

2016. Besides, using the average value from analyzing field samples from 2023, the correlation was used to calculate the Chl_a, CDOM, and Turb contents in the water.

ASTER data (Kääb [2002]) from the US Geological Survey was obtained using the digital elevation model (DEM), and topographic maps were also collected (scale of 1:50,000). Meteorological and hydrological data of the same period were concurrently collected.

In the year of 2020, the Ministry of Natural Resources and Environment updated climate change and sea level rise scenarios based on data sources, specific climate conditions of Vietnam, and products of climate models. The study applies two scenarios of RCP8.5 (the high scenario) and RCP4.5 (the medium scenario) to the study area based on climate change and sea level rise scenarios for Vietnam built corresponding to greenhouse gas emission scenarios (RCP), according to the new approach of the IPCC. Specifically: (1) According to RCP4.5, the average annual temperature nationwide at the beginning of the century (2020 - 2035) will commonly increase from 0.6 to 0.8oC, by the middle of the century. century (2046 – 2065) has a level increase by 1.3-1.7oC, by the end of the century (2080 - 2099) there will be an increase of 1.9-2.4oC; Annual rainfall at the beginning of the century tends to increase in most of the country, commonly by 5-10%, in the middle of the century it will increase by 5-15%, and by the end of the century it will have a distribution similar to the middle of the century. ; (2) For RCP8.5, the average annual temperature at the beginning of the century will generally increase by 0.8-1.1oC, and by the middle of the century there will be an increase of 1.8-2.3

oC , by the end of the century there will be an increase of 3.3-4.0oC; Annual rainfall has an increasing trend similar to the RCP4.5 scenario, notably by the end of the century the maximum increase could be over 20% in the study area (Ministry of Natural Resources and Environment (MONRE) [2020]).

2.3 Methodology

2.3.1 Standardized DEM ASTER

The DEM ASTER data (Kääb [2002]) with a resolution of thirty (30) meters needed to be corrected for missing information, such as hidden points, and depressions, and then regions with negative or equal values were removed. Thereafter, the resultant data was projected onto the Vietnam coordinate system (VN2000) and then superimposed onto the shape of the Nam Mu River basin. Finally, the data was converted into Grid format, which was compatible with computational usage in the SWAT model.

2.3.2 Land Cover Mapping

Samples were extracted using the Stratified Random Sampling method – SRS(Eq), which randomly selected a certain number of samples for each land cover object. Cochran's formula (Cochran [1977]) was used on the cloud computing platform, plus Google Earth Engine (GEE), to rectify the initial sample point size. The land cover classification was performed using the random forest (RF) method (Gíslason et al. [2006]; Thao and Sengchanh [2022]). For RF classification in this study, land cover objects, namely: forestland, cropland, wetland, residential land, other land, traffic system, borders and boundaries were all provided in the GEE environment. To assess the reliability of the land cover classification, the Kappa Khat error matrix method (Congalton [1991]) was used,

classification samples and random checkpoints were identified on Google Earth and generated in ArcGIS software. These samples with land sizes of 1 hectare, were converted into KML file format and loaded into Google Earth for visual image analysis. The land cover properties were then assigned to the checkpoints, and the number of these checkpoints was verified against topographic mapping data. The checking process of data reliability was conducted for the study area, using a specific number of sampling points, for each result.

The basin study area was divided into different land cover object types, covering the entire research area. The approach for classification depended on the natural conditions, specific to each country. For instance, in Vietnam, a classification system is applied based on land cover objects, as per the land use status map classification system. This system clusters land cover based on specific purposes, such as the forest layers and vegetation soil layers. Vietnam currently utilizes the classification regulations, as defined in Circular No. 27/2018/TT–BTNMT, dated 14th December 2018, Ministry of Natural Resources and Environment. The Circular guidelines focus on statistics, land inventory, and land use status mapping (Ministry of Natural Resources and Environment (MONRE) [2018]), and also, refer to the guideline in Intergovernmental Panel on Climate Change (IPCC) [2003].

2.3.3 Estimating Chl_a, CDOM, and Turb

To exact Chl_a, CDOM, and Turb in this study, multispectral data from Sentinel-2 were utilized to evaluate the water quality in specific zones, influencing the habitat of various species. The analysis was conducted using the GEE platform and a Machine Learning (ML) model (Hasan et al. [2021]; Kwong et al. [2022]).

Sentinel-2 SLC data were used to exact CDOM. Zhu et al. (2014) tested many algorithms with lake data from around the world and showed good performance of the green-to-red ratio globally. The green-to-red band ratio has demonstrated the best performance in retrieving lake CDOM from remote sensing (Brezonik et al. [2005]; Kutser et al. [2005]; Zhu et al. [2014]; Brezonik et al. [2015]). Therefore, the study has used the band 3 to band 4 ratios for estimating CDOM concentration from Sentinel-2 imagery (Kallio [1999]; Kutser et al. [2015]) with the formula is as follows:

$$CDOM = 537 \times e^{-2.93 \times \left(\frac{DN_{560nm}}{DN_{665nm}}\right)} \quad \text{(S2-L1C; Unit: mg/l) } \mathbf{(1)}$$

The product of Sentinel-2 at Level-2A is an orthoimage Bottom-Of-Atmosphere (BOA) corrected reflectance product. Sentinel-2 at Level-2A was processed by the steps of classification and an atmospheric correction of Top-Of-Atmosphere (TOA) from Level-1 orthoimage products. Then, Sentinel 2 at level 2A was provided information of surface reflectance in 12 spectral channels from central wavelength. The product Maximum Chlorophyll Index (MCI) was extracted from the level 2A images which is an indicator of the amount of chlorophyll content in water mass and thus a useful tool in the monitoring of algae blooms of inland waters. The bands selected for MCI index were the 442,5 nm, 560 nm, and 620 nm (Gower et al. [2008]). In addition, Potes et al. (2011, 2012, 2018) presented the methods to exact Chl_a and Turb with the formula as follows:

$$Chl_a = 4.23 \times \left(\frac{DN_{560nm}}{DN_{442.5nm}}\right)^{3.94} \quad \text{(S2-L2A; Unit: mg/m}^3\text{) } \mathbf{(2)}$$

$$Turb = 8.93 \times \left(\frac{DN_{560nm}}{DN_{442.5nm}} \right) - 6.39 \quad \text{(S2-L2A; Unit: NTU))} \textbf{ (3)}$$

2.3.4 SWAT Model Processing

The SWAT hydrological model was chosen for this study, due to its capacity to forecast and analyze the impacts of land cover changes on water resources – both in large and complex basins – over extended periods. The model comprises a major module that simulates runoff from rainfall and physical characteristics, coupled with a GIS interface that facilitates iterative computations with remote sensing data (Serrao et al. [2022]; Basu et al. [2022]). To simulate and forecast flows into the Ban Chat reservoir, various input data such as topography, land cover, roughness, hydro–meteorologic, and soil data were utilized. All the input data was processed in the required software formats before using for the calibrated model.

3 Results

3.1 LULC Monitoring

In the GEE platform, the RF algorithm was used for land cover objects' classification. Imagery bands of the study area and training area data (training data) are imported through the "raster" package. Based on the reliability assessment method, it was necessary to identify high-resolution image areas on Google Earth. Testing was conducted for the entire study area with a total of 238 sampling points for 2016, and 231 sampling points for 2024. The classification results achieved high values of reliability (Kappa coefficient values) as shown in Table 1.

Table 1: Results of reliability assessment for Sentinel-2 image classification.

N°	Year	Validation Kappa
1	Year 2016	79.20
2	Year 2024	82.51

Based on the Sentinel-2 image classification results, the land cover status map was developed to show the five thematic objects (forestland, cropland, wetland, residential land, and other land) which covered the entire research area is shown in Figure 2 (a, b).

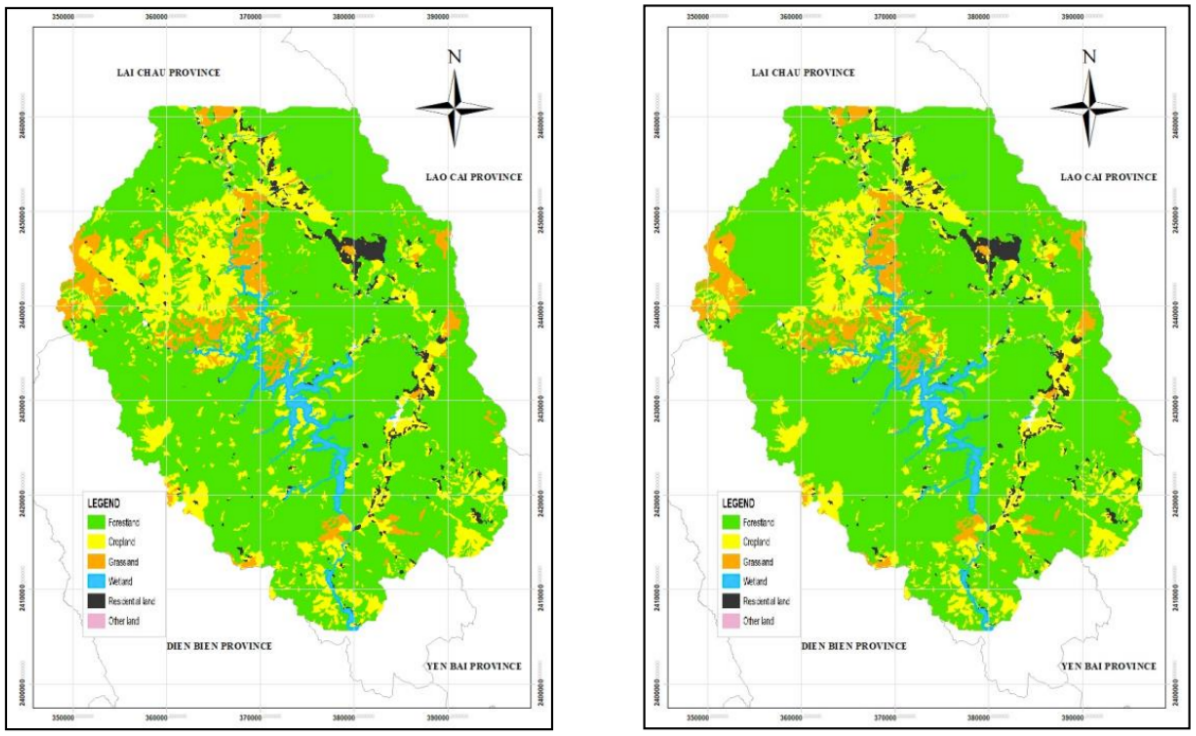

a) The year of 2016. b) The year of 2024

Figure 2: Illustration of the land cover map for the Ban Chat hydropower area, Northern Vietnam from Sentinel-2 imagery.

3.2 Land Cover Changes

Overlapping, separation, and establishment of land cover categories' changes, Table 2 shows the landcover status and change for the Cat Ba biosphere reserve for the period 2016–2024.

Table 2: Result calculation of land cover status and changes for the Ban Chat hydropower area.

N°	Category	2016 (ha)	2024 (ha)	The changes from 2016 to 2024 (ha)
1	Forestland	142,149.58	150,865.97	8,716.39
2	Cropland	23,925.28	14,913.04	-9,012.24
3	Grassland	4,936.20	4,265.78	-670.42
4	Wetland	1,164.69	1,166.99	2.30
5	Residential land	6,789.17	7,752.94	963.77
6	Other land	102.67	102.87	0.20
Total		179,067.59	179,067.59	0.00

3.3 Three Water Quality Indicators

In the Ban Chat reservoir, Sentinel-2 remote sensing data in Single Look Complex (SLC) format at level 1 was utilized during the period of 2016 - 2024 for monitoring CDOM concentration as shown in Figure 3, it showed that the average value of CDOM con centration for the five years ranged from

0.17 mg/l to 83.67 mg/l. In which, CDOM value as ranged from 0.17 mg/l and reached a peak of 83.67 mg/l in the year 2016; ranged from 0.83 mg/l and reached a peak of 43.13 mg/l in the year 2018; ranged from 3.14 mg/l and reached a peak of 32.42 mg/l in the year 2020; ranged from 2.37 mg/l and reached a peak of 79.58 mg/l in the year 2022; ranged from 2.09 mg/l and reached a peak of 44.66 mg/l in the year 2024.

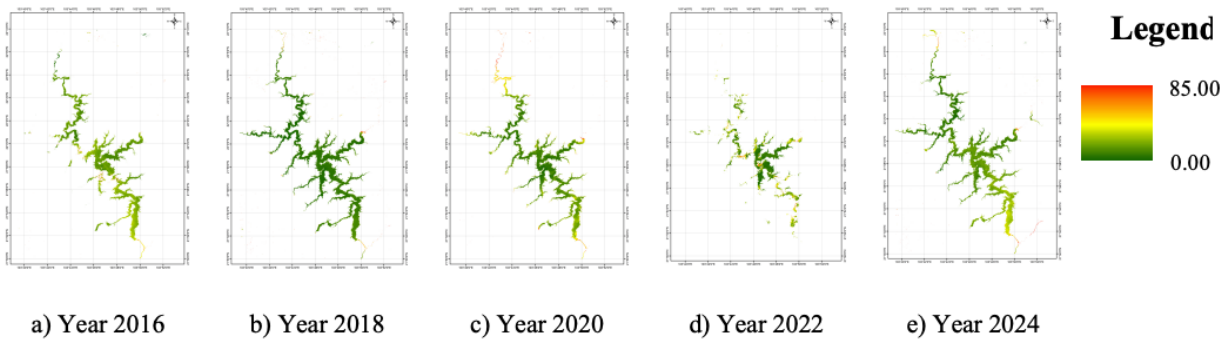

Figure 3: Illustration of CDOM concentration in the Ban Chat reservoir (Unit: mg/l).

In addition, Chl_a concentration was monitored from 2016 to 2024 using Sentinel-2 Level-2A data, shown in Figure 4. The average values of Chl_a concentration for these years ranged from 0.05 mg/m^3 to 24.79 mg/m^3, with peak values observed in different years.

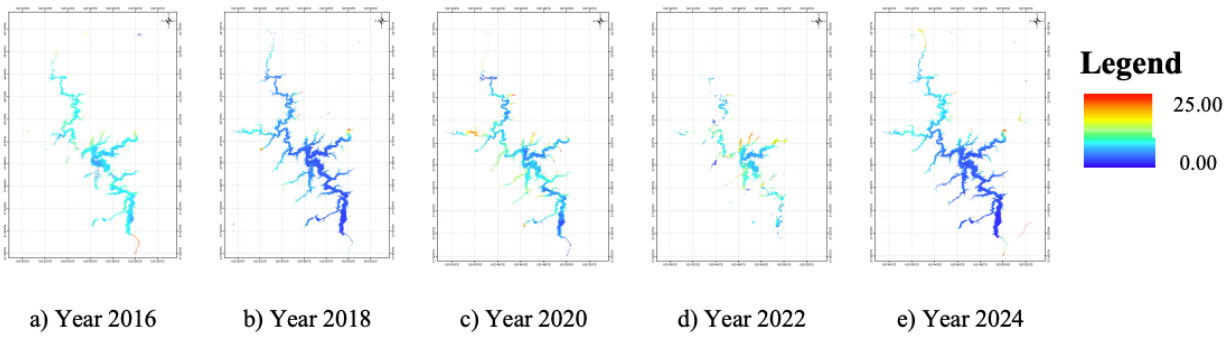

Figure 4: Illustration of Chl_a concentration in the Ban Chat reservoir (Unit: mg/m^3).

Furethermore, Sentinel-2 remote sensing data format at at Level-2A was utilized during the period of 2016 to 2024 for monitoring Turb concentration as shown in Figure 5, it showed that the average values of Turb concentration for the five years ranged from 0.05 NTU to 10.57 NTU. In which, the Turb value ranged from 0.48 NTU and reached a peak of 10.57 NTU in the year 2016; ranged from 0.67 NTU and reached a peak of 8.88 NTU in the year 2018; ranged from 0.18 NTU and reached a peak of 6.46 NTU in the year 2020; ranged from 0.05 NTU and reached a peak of 10.13 NTU in the year 2022; ranged from 0.44 NTU and reached a peak of 8.71 NTU in the year 2024.

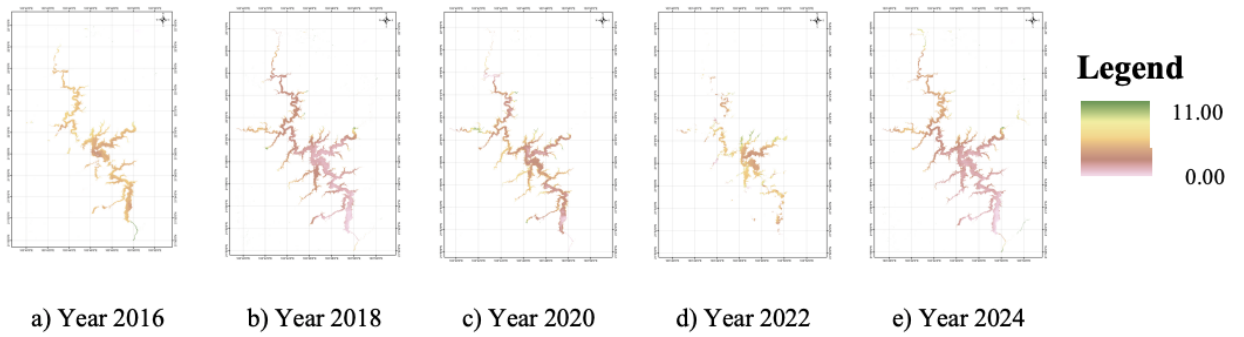

Figure 5: Illustration of Turb concentration in the Ban Chat reservoir (Unit: NTU).

3.4 Flood Flow Simulations into the Ban Chat Reservoir Under Local Climate Change Scenarios

After obtaining the complex input data set required for the SWAT model, the water flow at Ta Gia station on Nam Mu River was re-simulated. The flow calibration and verification process in using historical data series of 1981 – 1984 and 1986 – 1987, were carried out at Ta Gia hydrological station. In which, the data of flow rates playing a significant role in evaluating and calibrating the SWAT model. With the optimal parameter set, the SWAT model was run during the calibration phase, and a comparison was made between the actual measured flow data, versus the simulated flow. In this study, the flow simulation process improved, with the NSI index increasing to 0,818, the PBIA being 8,6%, and the resultant correlation coefficient R2 was 0,834. By using the parameter data set that was derived from the calibration process, the NSI index was 0,82, the PBIAS was 9,3%, and the resultant correlation coefficient was 0,83 (Table 3).

Based on the determined parameter set, the forecasting of flood flows and patterns into the Ban Chat reservoir was duly conducted.

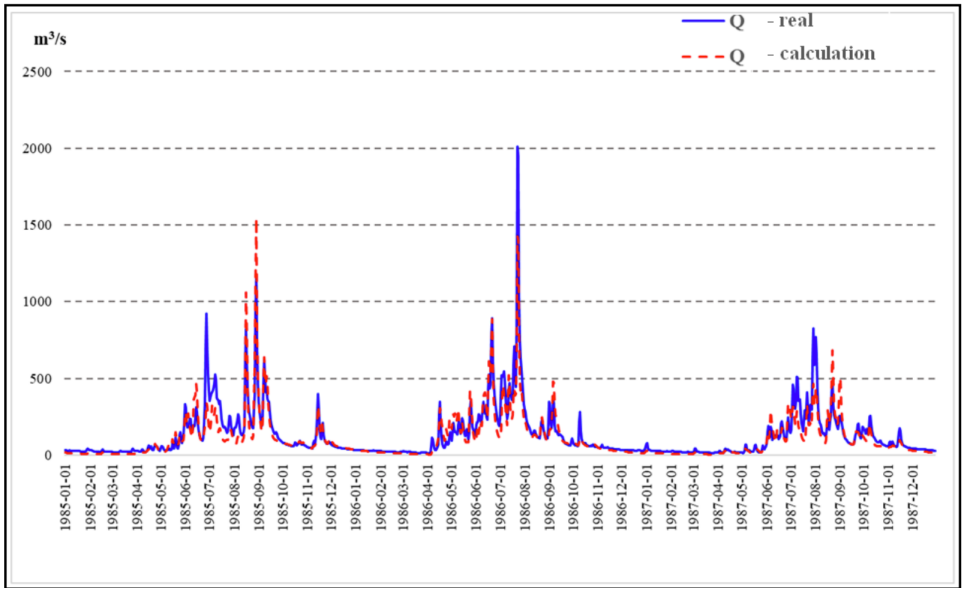

Figure 6: Monthly mean flow changes (l/s) under climate change scenarios compared to base flow scenarios (1986–2005).

Table 3: Flow simulation results: evaluation of calibration and verification periods.

Process	Period	R^2	NSE	PBIAS
Calibration	1981–1984	0.834	0.818	8.60
Testing	1986–1987	0.830	0.820	9.30

For flood flow simulations into the Ban Chat reservoir under local climate change scenarios, the change in flow rate within the Nam Mu River basin was simulated based on the actual measured daily average flows at the Ta Gia hydrological station, rainfall data from 5 stations (Pha Din, Sa Pa, Tam Duong, Mu Cang Chai, and Than Uyen); temperature data was obtained from 3 stations (Sin Ho, Tam Duong, and Than Uyen) within the basin and parapet area; rainfall data was duly extracted from the remote sensing imagery. By the typical annual flooding season of the Nam Mu River basin runs from April to September. Therefore, to simulate flood flows, it was crucial to assess the flow variations for each month, during the annual flooding season. The flood flow assessment results for the Ban Chat reservoir model simulations were done by using the already designated Vietnam local climate change scenarios (MONRE 2020), as follows:

3.4.1 Model Simulation Scenario of RCP 4.5

From 2020 to 2035, SWAT model simulation results showed that the average flow in flood season into the Ban Chat reservoir increased by 17,1%, compared to the baseline scenario of 1986–2005. The highest increase occurred during May with 25,1%; while the lowest rate was depicted during August, giving an increase of 11,7%.

From 2046 through 2065, statistical simulation results from the model showed that the average flows in flooding into the reservoir increased by 20,9%, compared to the baseline scenario of 1986–2005. The highest increase was depicted in May with 29,7 %; while the lowest spike of 14,6% was experienced in August.

Additionally, from 2080 to 2099, SWAT model results showed that the flooding season flows increased more than the above two periods for the same RCP 4.5 scenario. Consequently, the average flows during the flooding season increased by 26,1% compared to the base scenario, while May and June depicted the highest increase in flow rates, with 35,7% and 36%, respectively. The lowest increase in flooding was depicted in April, giving a percentage of just 18,7%.

3.4.2 Model Simulation Scenario of RCP 8.5

From 2020 to 2035, the SWAT model simulation results clearly showed that the average flows in the flood seasons, into the Ban Chat reservoir tended to decrease by 0,5%, compared to the baseline scenario. The significant decrease was depicted in April with 2,9%; while the lowest (0,3%) was experienced in June. However, the month of May demonstrated an upward trend of 2,8

In addition, for the simulation period of 2046–2065, the calibrated model results showed that the average flows in flooding into the Ban Chat reservoir increased by 12,9%; compared to the baseline scenario of 1986 – 2005. Also, the greatest increase was during May, depicting a value of 19,6%. Consequently, the lowest growth rate was during August, giving the value of 8,6%.

Furthermore, the period of 2080–2099 provided model simulation results that showed flood spiked with an increased rate of 45,7%, compared to the baseline scenario. Consequently, the month of April gave the largest increase of 65,7%, while June depicted a 60,2% increase. The month of August depicted the lowest increase of just 33,4%.

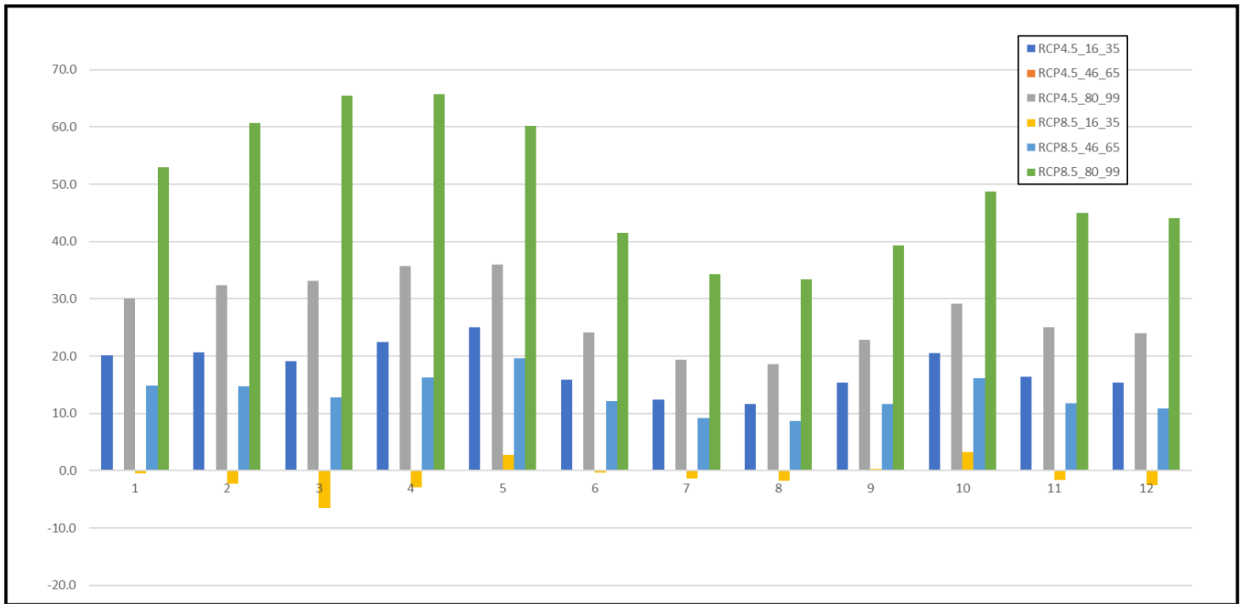

Figure 7: Monthly mean flow changes (l/s) under climate change scenarios compared to base flow scenarios (1986–2005).

4 Discussion

The remote sensing images show that forestland, grassland, cropland, wetland, residential land, and other land usages, have different spectral characteristics (Yu et al. 2017). In this study, five land cover categories proposed are focused on and applied to the Ban Chat reservoir area. Remote sensing data are used to estimate the land cover and to identify the characteristics of land cover objects based on the afforestation efforts in Vietnam as well as three water quality indicators in the study area.

The classification process revealed that grassland and forestland were easily confused due to their similar spectral characteristics. At the same time, residential and vacant land were classified as "other" land types, as noted by Yifan et al. [2018]. The reliability assessment (Table 1) indicated that the confusion between grassland and forestland was due to their intermixing in certain areas, resulting in spectral similarity. Additionally, the presence of mixed populations with vegetation made classification more challenging, as this source of error is difficult to avoid even with manual interpretation. In some cases, these errors may be acceptable, even with traditional classification methods. In the study area, most of the land cover objects did not change much, only the increased change of forestland area (8.716,39 ha) which was replaced by the decreased change in grass and bushes (9.012,24 ha). This is consistent with the afforestation strategy in Vietnam.

The red areas on the water maps (Figures 3 and 4) show that some indicators exceed the threshold. Although there were instances where water and air quality indicators exceeded permissible limits, the average values for each year confirmed that indices such as Chl_a, CDOM, and Turb in the study area were within the prescribed limit thresholds. Therefore, after a comparison of water quality indicators with Carlson and Simpson [1996] and Ministry of Natural Resources and Environment (MONRE) [2022]. The three water quality indicators were consistent with the results of the conservation progress of Ban Chat reservoir in Vietnam. There are similarities in the change trends

of Chl_a, CDOM, and Turb in the study area. The results showed that the Ban Chat hydropower area in Northern Vietnam is being effectively preserved, showing no signs of significant degradation.

This dataset served as an important input parameter for running the SWAT hydrological model, and is a valuable tool for estimating river flow, as evidenced by the effectiveness of satellite-based measurements and highly accurate sensors, as noted by Wu et al. [2017].

Climate change has a significant impact on water resources in vulnerable international river basins, particularly concerning upstream runoff variability Brekke et al. 2007; Yang et al. 2019). To assess the impact of climate change on flood flow during the period from 2020 to 2035, 2045 to 2065, and 2080 to 2099, two scenarios were chosen: high emission RCP 8.5 and average emission RCP 4.5. The results of the flood flow change calculations showed an increasing trend during most periods. The period of 2080 to 2099 (RCP 8.5 scenario) had the highest increase in flood season flow at 45,7%, compared to the baseline scenario, while the lowest increase was observed from 2045 to 2065 (RCP 8.5 scenario) at a rate of 12,9%. However, during the period 2020 to 2035 if applied the RCP 8.5 scenario, the flood season flow tended to decrease by 0,5%, compared to the baseline scenario. Therefore, the impact of climate change on flood flows to Ban Chat reservoir exhibited significant variation during the flood season across different periods, as depicted by the climate change scenarios of Vietnam by the Ministry of Natural Resources and Environment (MONRE) [2020].

Acknowledgments

Many thanks must go to our colleagues, the research group of the Vietnam National Remote Sensing Department, who have generously given their time, suggestions, data, and materials in order to bring this task to fruition.

References

R. Alvarez, R. Bonifaz, R. S. Lunetta, C. Garcia, G. Gomez, R. Castro, A. Bernal, and A. L. Cabrera. Multitemporal landcover classification of mexico using landsat mss imagery. *International Journal of Remote Sensing*, 24:2501–2514, 2003. doi: 10.1080/01431160210153066.

T. R. B. T. Aranha, J. M. Martinez, E. P. Souza, M. U. G. Barros, and E. S. P. R. Martins. Remote analysis of the chlorophyll-a concentration using sentinel-2 msi images in a semiarid environment in northeastern brazil. *Water*, 14:451, 2022. doi: 10.3390/w14030451.

Anne Ave and Krista Alikas. Retrieval of chlorophyll *a* from sentinel-2 msi data for the european union water framework directive reporting purposes. *Remote Sensing*, 11(1):64, 2018. doi: 10.3390/rs11010064.

A. S. Basu, L. W. Gill, F. Pilla, and B. Basu. Assessment of variations in runoff due to land cover changes using the swat model in an urban river in dublin, ireland. *Sustainability*, 14(1):534, 2022. doi: 10.3390/su14010534.

F. Bioresita, C. B. Pribadi, H. S. Firdaus, T. Hariyanto, and A. Puissant. The use of sentinel-2 imagery for total suspended solids (tss) estimation in porong river, sidoarjo. *ELIPSOIDA (Journal Geodesi dan Geomatika)*, 1(1):1–6, 2018. doi: 10.14710/elipsoida.2018.2726.

P. Brezonik, K. D. Menken, and M. Bauer. Landsat-based remote sensing of lake water quality characteristics, including chlorophyll and colored dissolved organic matter (cdom). *Lake and Reservoir Management*, 21:373–382, 2005. doi: 10.1080/07438140509354442.

P. Brezonik, L. G. Olmanson, J. C. Finlay, and M. Bauer. Factors affecting the measurement of cdom by remote sensing of optically complex inland waters. *Remote Sensing of Environment*, 157:199–215, 2015. doi: 10.1016/j.rse.2014.04.033.

R. P. Bukata, J. E. Bruton, J. H. Jerome, S. C. Jain, and H. H. Zwick. Optical water quality model of lake ontario. 2: Determination of chlorophyll a and suspended mineral concentrations of natural waters from submersible and low altitude optical sensors. *Applied Optics*, 20:1704–1714, 1981. doi: 10.1364/AO.20.001704.

R. E. Carlson and J. Simpson. *A Coordinator's Guide to Volunteer Lake Monitoring Methods*. North American Lake Management Society, Madison, WI, 1996.

W. G. Cochran. *Sampling Techniques*. John Wiley and Sons, New York, 3rd edition, 1977.

R. G. Congalton. A review of assessing the accuracy of classification of remotely sensed data. *Remote Sensing of Environment*, 37:35–46, 1991. doi: 10.1016/0034-4257(91)90048-B.

D. Datta. Assessment of mangrove management alternatives in village-fringe forests of indian sunderbans: resilient initiatives or short-term nature exploitations. *Wetlands Ecology and Management*, 26:399–413, 2018. doi: 10.1007/s11273-017-9582-7.

A. G. Dekker, R. J. Vos, and S. W. M. Peters. Comparison of remote sensing data, model results and in situ data for total suspended matter (tsm) in the southern frisian lakes. *Science of The Total Environment*, 268:197–214, 2001. doi: 10.1016/S0048-9697(00)00679-3.

Y. Du, Y. Zhang, F. Ling, Q. Wang, W. Li, and X. Li. Water bodies' mapping from sentinel-2 imagery with modified normalized difference water index at 10-m spatial resolution produced by sharpening the swir band. *Remote Sensing*, 8:354, 2016. doi: 10.3390/rs8040354.

European Space Agency (ESA). Sentinel-2 user handbook. Technical report, ESA, Paris, France, 2015. URL https://sentinel.esa.int/documents/247904/685211/Sentinel-2_User_Handbook.

S. E. Franklin and M. A. Wulder. Remote sensing methods in medium spatial resolution satellite data land cover classification of large areas. *Progress in Physical Geography*, 26:173–205, 2002. doi: 10.1191/0309133302pp332ra.

C. Giardino, V. E. Brando, A. G. Dekker, N. Strömbeck, and G. Candiani. Assessment of water quality in lake garda (italy) using hyperion. *Remote Sensing of Environment*, 109:183–195, 2007. doi: 10.1016/j.rse.2006.12.017.

A. Gitelson, G. Garbuzov, F. Szilagyi, K. H. Mittenzwey, A. Karnieli, and A. Kaiser. Quantitative remote sensing methods for real-time monitoring of inland waters quality. *International Journal of Remote Sensing*, 14:1269–1295, 1993. doi: 10.1080/01431169308953956.

A. A. Gitelson. The peak near 700 nm on radiance spectra of algae and water: Relationships of its magnitude and position with chlorophyll concentration. *International Journal of Remote Sensing*, 13:3367–3373, 1992. URL https://calmit.unl.edu/people/agitelson2/pdf/52_IJRS-1992(3367-3373).pdf.

J. F. R. Gower, S. King, and P. Goncalves. Global monitoring of plankton blooms using meris mci. *International Journal of Remote Sensing*, 29:6209–6216, 2008. doi: 10.1080/01431160802178110.

P. Ó. Gíslason, J. A. Benediktsson, and J. R. Sveinsson. Random forests for land cover classification. *Pattern Recognition Letters*, 27(4):294–300, 2006. doi: 10.1016/j.patrec.2005.08.011.

H. T. T. Hanh. Using gis and swat model to assess soil and water resources in upstream srepok watershed, dak lak province. Master's thesis, Bach Khoa University, Ho Chi Minh City, Vietnam, 2010.

S. H. Hasan, A. N. M. Al-Hameedawi, and H. S. Ismael. Using google earth engine development environment for remote sensing image analysis, al shuwija marsh case study. *Journal of Physics: Conference Series*, 1973:012192, 2021. doi: 10.1088/1742-6596/1973/1/012192.

L. Q. Hung. Research in combination between remote sensing technology and numerical model to build flood flow scenarios to reservoirs for downstream impact prevention and mitigation in the case of an incident. Technical report, Vietnam Ministry of Natural Resources and Environment, 2021. Code: TNMT.08/16–20.

L. Q. Hung, D. T. Giang, and N. N. Quang. Super resolution method approach for vietnam remote sensing imagery. *International Journal of Remote Sensing Applications (IJRSA)*, 6:118–126, 2016.

L. Q. Hung, T. Asaeda, and V. T. P. Thao. Carbon emissions in the field of land use, land use change, land forestry in the vietnam mainland. *Wetlands Ecology and Management*, 29:315–329, 2021. doi: 10.1007/s11273-021-09789-6.

P. D. Hunter, A. N. Tyler, L. Carvalho, G. A. Codd, and S. C. Maberly. Hyperspectral remote sensing of cyanobacterial pigments as indicators for cell populations and toxins in eutrophic lakes. *Remote Sensing of Environment*, 114:2705–2718, 2010. doi: 10.1016/j.rse.2010.06.006.

Intergovernmental Panel on Climate Change (IPCC). Good practice guidance for land use, land–use change and forestry. Technical report, ICPCC, 2003. URL https://www.ipcc.ch/site/assets/uploads/2018/03/GPG_LULUCF_FULLEN.pdf.

A. S. Jasrotia, S. D. Dhiman, and S. P. Aggarwal. Rainfall–runoff and soil erosion modeling using remote sensing and gis technique—a case study of tons watershed. *Journal of the Indian Society of Remote Sensing*, 30:167–180, 2002. doi: 10.1007/BF02990649.

J. R. Jensen. *Remote Sensing of the Environment: An Earth Resource Perspective*. Pearson Prentice Hall, Upper Saddle River, NJ, USA, 2nd edition, 2000.

J. R. Jensen. *Introductory Digital Image Processing: A Remote Sensing Perspective*. Prentice Hall, Upper Saddle River, 3rd edition, 2005.

K. Kallio. Absorption properties of dissolved organic matter in finnish lakes. *Proceedings of the Estonian Academy of Sciences Biology Ecology*, 48:75–83, 1999. URL https://thuvien.huce.edu.vn/kiposdata1/baotapchi/Tapchinuocngoai/Water%20Research/2016/Water%20research,Vol.102/PDF/Water%20research,Vol.102,%20A6.pdf.

K. Kallio, T. Kutser, T. Hannonen, S. Koponen, J. Pulliainen, J. Vepsäläinen, and T. Pyhälahti. Retrieval of water quality from airborne imaging spectrometry of various lake types in different seasons. *Science of The Total Environment*, 268:59–77, 2001. doi: 10.1016/S0048-9697(00)00685-9.

R. Katlane, C. Dupouy, E. B. Kilani, and J. C. Berges. Estimation of chlorophyll and turbidity using sentinel 2a and eo1 data in kneiss archipelago gulf of gabes, tunisia. *International Journal of Geosciences*, 11(10):708–728, 2020. doi: 10.4236/ijg.2020.1110035.

T. Kutser, D. C. Pierson, K. Kallio, A. Reinart, and S. Sobek. Mapping lake cdom by satellite remote sensing. *Remote Sensing of Environment*, 94:535–540, 2005. doi: 10.1016/j.rse.2004.11.009.

T. Kutser, C. Verpoorter, B. Paavel, and L. J. Tranvik. Estimating lake carbon fractions from remote sensing data. *Remote Sensing of Environment*, 157:138–146, 2015. doi: 10.1016/j.rse.2014.05.020.

T. Kutser, B. Paavel, C. Verpoorter, M. Ligi, T. Soomets, K. Toming, and G. Casal. Remote sensing of black lakes and using 810 nm reflectance peak for retrieving water quality parameters of optically complex waters. *Remote Sensing*, 8:497, 2016. doi: 10.3390/rs8060497.

I. H. Y. Kwong, K. Frankie, K. Wong, and T. Fung. Automatic mapping and monitoring of marine water quality parameters in hong kong using sentinel-2 image time-series and google earth engine cloud computing. *Frontiers in Marine Science*, 9:871470, 2022. doi: 10.3389/fmars.2022.871470.

A. Kääb. Monitoring high-mountain terrain deformation from repeated air- and spaceborne optical data: Examples using digital aerial imagery and aster data. *ISPRS Journal of Photogrammetry and Remote Sensing*, 57:39–52, 2002. doi: 10.1016/S0924-2716(02)00114-4.

M. Li, S. Zang, B. Zhang, S. Li, and C. Wu. A review of remote sensing image classification techniques: the role of spatio-contextual information. *European Journal of Remote Sensing*, 47: 389–411, 2014. doi: 10.5721/EuJRS20144723.

D. Lu and Q. Weng. A survey of image classification methods and techniques for improving classification performance. *International Journal of Remote Sensing*, 28(5):823–870, 2007. doi: 10.1080/01431160600746456.

Ministry of Natural Resources and Environment (MONRE). Circular no. 27/2018/tt–btnmt: Regulations on statistics, inventory land, and current land use mapping, 2018. Available online: https://thuvienphapluat.vn/van-ban/Bat-dong-san/Thong-tu-27-2018-TT-BTNMT-thong-ke-kiem-ke-dat-dai-va-lap-ban-do-hien-trang-su-dung-dat-404794.aspx (in Vietnamese).

Ministry of Natural Resources and Environment (MONRE). Climate change and sea level rise scenarios for vietnam. Technical report, Vietnam Publishing House of Natural Resource, Environment and Cartography, Hanoi, Vietnam, 2020. URL http://www.imh.ac.vn/files/doc/2017/CCS%20final.compressed.pdf.

Ministry of Natural Resources and Environment (MONRE). National report on water resources. Technical report, Ministry of Natural Resources and Environment, Hanoi, Vietnam, 2022. Available online: http://dwrm.gov.vn/index.php?language=vi&nv=download&op=Sa-ch-Ta-i-lieu-tham-kha-o/BAO-CAO-TAI-NGUYEN-NUOC-QUOC-GIA-GIAI-DOAN-2016-2021 (accessed on 5 April 2023). (In Vietnamese).

Ministry of Natural Resources and Environment (MONRE). National technical regulation on surface water quality no qcvn 08:2023/btnmt, 2023.

M. K. Mukhtar, S. Supriatna, and M. D. M. Manessa. The validation of water quality parameter algorithm using landsat 8 and sentinel-2 image in palabuhanratu bay. *IOP Conference Series: Earth and Environmental Science*, 846:012022, 2021. doi: 10.1088/1755-1315/846/1/012022.

D. H. Nam, K. Udo, and A. Mano. Climate change impacts on runoff regimes at a river basin scale in central vietnam. *Terrestrial, Atmospheric and Oceanic Sciences*, 23(5):541–551, 2012. doi: 10.3319/TAO.2012.05.03.03(WMH).

T. H. D. Nguyen, K. D. Phan, H. T. T. Nguyen, S. N. Tran, T. G. Tran, B. L. Tran, and T. N. Doan. Total suspended solid distribution in hau river using sentinel 2a satellite imagery. *ISPRS Annals*

of the Photogrammetry, Remote Sensing and Spatial Information Sciences, VI-3/W1-2020:91–97, 2020. doi: 10.5194/isprs-annals-VI-3-W1-2020-91-2020.

N. Y. Nhu and N. T. Son. Swat model application to investigate the effects of land use scenarios on flow in river basin ben hai. *VNU Journal of Science*, 3S:492–498, 2009.

L. G. Olmanson, M. E. Bauer, and P. L. Brezonik. A 20-year landsat water clarity census of minnesota's 10,000 lakes. *Remote Sensing of Environment*, 112:4086–4097, 2008. doi: 10.1016/j.rse.2007.12.013.

A. Ostfeld, S. Barchiesi, M. Bonte, and C. Collier. Climate change impacts on river basin and freshwater ecosystems: Some observations on challenges and emerging solutions. *Journal of Water and Climate Change*, 3(3):171–184, 2012. doi: 10.2166/wcc.2012.006.

N. Pahlevan, B. Smith, J. Schalles, C. Binding, Z. Cao, R. Ma, K. Alikas, K. Kangro, D. Gurlin, N. Ha, B. Matsushita, W. Moses, S. Greb, M. K. Lehmann, M. Ondrusek, N. Oppelt, and R. Stumpf. Seamless retrievals of chlorophyll-a from sentinel-2 (msi) and sentinel-3 (olci) in inland and coastal waters: A machine-learning approach. *Remote Sensing of Environment*, 240: 111604, 2020. doi: 10.1016/j.rse.2019.111604.

A. Pietroniro and T. D. Prowse. Applications of remote sensing in hydrology. *Hydrological Processes*, 16:1537–1541, 2002. doi: 10.1002/hyp.1018.

M. Potes, M. J. Costa, J. C. B. Silva, A. M. Silva, and M. Morais. Remote sensing of water quality parameters over alqueva reservoir in the south of portugal. *International Journal of Remote Sensing*, 32:3373–3388, 2011. doi: 10.1080/01431161003747513.

M. Potes, M. J. Costa, and R. Salgado. Satellite remote sensing of water turbidity in alqueva reservoir and implications on lake modelling. *Hydrology and Earth System Sciences*, 16:1623–1633, 2012. doi: 10.5194/hess-16-1623-2012.

M. Potes, G. Rodrigues, A. M. Penha, M. F. Novais, M. J. Costa, R. Salgado, and M. M. Morais. Use of sentinel 2 – msi for water quality monitoring at alqueva reservoir, portugal. *Proceedings of the International Association of Hydrological Sciences*, 380:73–79, 2018. doi: 10.5194/piahs-380-73-2018.

A. Rango. Application of remote sensing methods to hydrology and water resources. *Hydrological Sciences Journal*, 39:309–320, 1994. doi: 10.1080/02626669409492752.

A. P. Riza, P. S. Budi, A. A. Saharani, D. G. Hutagalung, and R. Ramadhan. Temporal detection of total suspended solid (tss) distribution in the southern area of obi island. *BIO Web of Conferences*, 106:04012, 2024. doi: 10.1051/bioconf/202410604012.

R. M. B. Santos, L. F. S. Fernandes, J. P. Moura, M. G. Pereira, and F. A. L. Pacheco. The impact of climate change, human interference, scale and modelling uncertainties on the estimation of aquifer properties and river flow components. *Journal of Hydrology*, 519(Part B):1297–1314, 2014. doi: 10.1016/j.jhydrol.2014.09.001.

E. A. de O. Serrao, M. T. Silva, T. R. Ferreira, L. C. P. de Ataide, C. A. dos Santos, A. M. M. de Lima, V. P. R. da Silva, F. A. S. de Sousa, and D. J. C. Gomes. Impacts of land use and land cover changes on hydrological processes and sediment yield determined using the swat model. *International Journal of Sediment Research*, 37(1):54–69, 2022. doi: 10.1016/j.ijsrc.2021.04.002.

J. Sheffield, E. F. Wood, M. Pan, H. Beck, G. Coccia, A. Serrat-Capdevila, and K. Verbist. Satellite remote sensing for water resources management: potential for supporting sustainable development

in data-poor regions. *Water Resources Research*, 54(12):9724–9758, 2018. doi: 10.1029/2017WR022437.

L. C. Smith. Satellite remote sensing of river inundation area, stage, and discharge: a review. *Hydrological Processes*, 11:1427–1439, 1997. doi: 10.1002/(SICI)1099-1085(199708)11:10<1427::AID-HYP473>3.0.CO;2-S.

V. T. P. Thao and S. Sengchanh. Building ability of land cover map from sentinel-2 remote sensing data using the random forest classification method on the cloud computing platform. *Vietnam Journal of Surveying and Mapping Sciences*, 52:26–35, 2022. doi: 10.54491/jgac.2022.52.594.

V. T. P. Thao, D. T. Giang, and L. V. Anh. Reliability assessment of land subsidence monitoring results using psi technique in ho chi minh city, vietnam. *International Journal of Environmental Studies*, 81(2):881–895, 2024. doi: 10.1080/00207233.2024.2324623.

The United States Geological Survey (USGS). Landsat satellite missions, 2024. URL https://earthexplorer.usgs.gov/.

T. K. Trang. Application of gis and swat model to assess the impact of land use change on environment in di an district, binh duong province. Master's thesis, Nong Lam University, Vietnam, 2009.

N. T. Tuan, P. V. Tuan, N. V. Quy, and H. T. P. Nhung. Using sentinel 2 satellite images and machine learning algorithm to establish the current status map of forests in bu dang district, binh phuoc province. *Can Tho University Science Magazine*, 58(6B):150–163, 2022. doi: 10.22144/ctu.jvn.2022.254.

T. V. Ty, K. Sunada, and Y. Ichikawa. Water resources management under future development and climate change impacts in the upper srepok river basin, central highlands of vietnam. *Water Policy*, 14(5):725–745, 2012. doi: 10.2166/wp.2012.095.

P. D. T. Van, I. Popescu, A. Van Griensven, D. P. Solomatine, N. H. Trung, and A. Green. A study of the climate change impacts on fluvial flood propagation in the vietnamese mekong delta. *Hydrology and Earth System Sciences*, 16:4637–4649, 2012. doi: 10.5194/hess-16-4637-2012.

F. A. Vertucci and G. E. Likens. Spectral reflectance and water quality of adirondack mountain region lakes. *Limnology and Oceanography*, 34:1656–1672, 1989. URL https://aslopubs.onlinelibrary.wiley.com/doi/pdf/10.4319/lo.1989.34.8.1656.

K. Västilä, M. Kummu, C. Sangmanee, and S. Chinvanno. Modelling climate change impacts on the flood pulse in the lower mekong floodplains. *Journal of Water and Climate Change*, 1(1):67–86, 2010. doi: 10.2166/wcc.2010.008.

Y. Wang. Advances in remote sensing of flooding. *Water*, 7(11):6404–6410, 2015. doi: 10.3390/w7116404.

Q. Wu, C. Lane, M. Vanderhoof, and C. Song. Remote sensing of climate change and water resources. *Remote Sensing*, 9(5):475, 2017.

W. Yang, D. Long, and P. Bai. Impacts of future land cover and climate changes on runoff in the mostly afforested river basin in north china. *Journal of Hydrology*, 570:201–219, 2019. doi: 10.1016/j.jhydrol.2018.12.055.

C. Yifan, L. Long, C. Longqian, Z. Yu, C. Liang, Z. Xisheng, and Y. Xiaoyan. Land-use carbon emissions estimation for the yangtze river delta urban agglomeration using 1994–2016 landsat image data. *Remote Sensing*, 10(9):1334, 2018. doi: 10.3390/rs10091334.

W. Yu, Z. Xicun, L. Cheng, G. Xiaoyan, Y. Xinyang, C. Chunyan, and S. Houxing. Applications of hyperspectral remote sensing in ground object identification and classification. *Advances in Remote Sensing*, 6(3):201–211, 2017. doi: 10.4236/ars.2017.63015.

R. Zhai, F. Tao, U. Lall, B. Fu, J. Elliott, and J. Jägermeyr. Larger drought and flood hazards and adverse impacts on population and economic productivity under 2.0 than 1.5°c warming. *Earth's Future*, 8(8):e2019EF001398, 2020. doi: 10.1029/2019EF001398.

W. Zhu, Q. Yu, Y. Q. Tian, B. L. Becker, T. Zheng, and H. J. Carrick. An assessment of remote sensing algorithms for colored dissolved organic matter in complex freshwater environments. *Remote Sensing of Environment*, 140:766–778, 2014. URL https://www.geo.umass.edu/faculty/yu/2014ZhuRSE.pdf.